$CeAuGa_3$的力学性质及磁性的第一性原理计算

程耀世，刘本琼
(中国工程物理研究院核物理与化学研究所，绵阳 621999)

摘　要：本文基于第一性原理计算研究了铈基金属间化合物 $CeAuGa_3$ 的结构性质与力学稳定性，获得了弹性常数、宏观弹性参数(包括体弹模量、剪切模量、杨氏模量、泊松比)以及声子色散曲线，结果表明 I4mm 结构不仅力学稳定，且动力学稳定. 通过计算铈离子之间的自旋交换相互作用，我们分析了 $CeAuGa_3$ 几种可能的有序自旋态，并发现该材料的基态可能是铁磁结构. 位于 *ab* 面内的第一近邻和第二近邻的正(铁磁)交换耦合起主导作用，而位于相邻平面的铈离子之间的第三近邻铁磁相互作用则非常微弱.

关键词：弹性常数；自旋交换相互作用；声子色散；第一性原理计算
中图分类号：O469　　**文献标识码**：A　　DOI：10.19907/j.0490-6756.2021.054005

Mechanical and magnetic properties of $CeAuGa_3$ from first-principles calculations

CHENG Yao-Shi, *LIU Ben-Qiong*
(Institute of Nuclear Physics and Chemistry, China Academy of Engineering Physics, Mianyang 621999, China)

Abstract: In this paper, the structural properties and the mechanical stability of Ce-based intermetallic $CeAuGa_3$ are studied based on the first-principles calculations. The full sets of elastic constants, the associated macroscopic elastic parameters (bulk, shear and Young's moduli, Poisson ratio), and phonon dispersion have been determined, indicating that the I4mm structure is both mechanically and dynamically stable. By calculating the spin exchange interaction between cerium ions, we have analyzed several possible ordered spin states of $CeAuGa_3$, and found that the ground state of $CeAuGa_3$ prefers to be ferromagnetic ordering. The positive (ferromagnetic) exchange couplings within each *ab* layer play a dominant role, while the third nearest neighbour ferromagnetic interaction between adjacent *ab* layers of Ce ions is relatively weak.

Keywords: Elastic constants; Spin exchange interactions; Phonon dispersion; First-principles calculations

1　Introduction

It is very attractive to study the Cerium-based intermetallic compounds, since they exhibit lots of interesting behaviors resulting from the interplay between the single-impurity Kondo effect and the Ruderman-Kittel-Kasuya-Yosida (RKKY) interactions. Especially, the stoichiometric compounds with the general formula $CeTX_3$ or CeT_yX_{4-y} (T is a transition metal, X is a simple metal) have

收稿日期：2021-03-07
基金项目：国家自然科学基金面上项目(11875238)
作者简介：程耀世(1996－)，男，山西大同人，硕士研究生，主要研究铈基材料的中子散射及相关理论计算.
通讯作者：刘本琼. E-mail：liubenqiong@caep.cn

recently received great attention, because important new features have been observed in addition to their novel ground state properties which have been studied extensively. For examples, there is relatively low Cu-Al atomic site disorder[1-2] in $CeCuAl_3$, which leads to the previous argument about its true crystal structure of either the ThCr_2Si_2-type[3] or the $BaNiSn_3$-type[4-5], and indeed can influence the electronic properties. $CeNiGe_3$ undergoes antiferromagnetic (AFM) phase transition below $T_N = 5.5$ K at ambient pressure and exhibits a quantum critical point at about 6～7 GPa. The superconductivity in this material exists in a wide range of 1.7～9.3 GPa[6-7], and the spin-fluctuations may be not the hidden mechanism at the lower pressure region. Kimura *et al.*[8] presented an unconventional pressure-induced superconductor $CeRhSi_3$, where the superconductivity and the AFM state coexist, with $T_N = 1.6$ K at ambient pressure. Another similar example is the antiferromagnet $CeIrSi_3$, where superconductivity appears in 1.8～3.5 GPa[9]. Although most of $CeTX_3$ compounds show AFM ordering at low temperature, $CeAgAl_3$[10] is a scarce example of ferromagnetic compound with $T_C = 3.0$ K. Further, selected members of this class offer the new insights that magnetoelastic coupling could result in the formation of a bound state between low-lying phonons and a crystal electric field (CEF) excitation. Adroja *et al.* first reported the presence of an additional magnetic excitation in the neutron spectra of $CeCuAl_3$ measured in the paramagnetic phase[11], which cannot be explained by a pure CEF model. By generalizing the theoretical model proposed by Thalmeier and Fulde for the cubic system $CeAl_2$[12-13] to the tetragonal point-group symmetry, a satisfactory interpretation for the magnetic inelastic neutron scattering spectra of $CeCuAl_3$ can be achieved. In recent studies of $CeAuAl_3$[14-15], except for the pronounced vibronic bound state, a well-resolved anti-crossing of the CEF excitations with the acoustic phonon branch at zero magnetic field has also been observed by neutron scattering.

In this work, we present detailed first-principles calculations of the structural and mechanical properties of $CeAuGa_3$, which has been rarely studied and may behave qualitatively similarly to $CeAuAl_3$. Total energies of different spin arrangements of $CeAuGa_3$ have been compared, and our results show that the total energy of ferromagnetic (FM) configuration is indeed the lowest, *i.e.*, in the ground state a FM ordering state is favored. By further analyzing the paths of spin exchange coupling, it is found that all the spin exchange interactions are positive ferromagnetic type. The couplings between the Ce ions parallel to the *ab* plane are comparable, while the third-nearest-neighbour coupling between the Ce ions within adjacent layers is relatively weak.

2 Computational methods

Several different spin configurations of $CeAuGa_3$ were examined by evaluating the exchange coupling constants between the Ce ions via mapping analysis based on first principles calculations. The Vienna *ab initio* simulation package (VASP)[16-18] was used, with the standard frozen-core projector augmented wave (PAW) method, and the generalized gradient approximations (GGA) for the exchange and correlation corrections. The plane-wave cutoff energy was tested and set to 550 eV. According to the Monkhorst-Pack scheme, the *k*-point meshes in the Brillouin zone were sampled by 10×10×5 grids. For the elastic property calculations, a denser *k*-mesh sampling of 12×12×6 was adopted for accuracy. In order to obtain the phonon dispersion, Phonopy code[19] was used and a 2×2×2 supercell was constructed with the *k*-point meshes of 4×4×4. Other parameters included a convergence criterion of the Hellmann-Feynman force of 0.01 eV/Å, and 10^{-8} eV for the total energy tolerance.

3 Discussion

3.1 Spin exchange parameters

According to Mock *et al.*[20], $CeAuGa_3$ crystallizes in the non-centrosymmetric $BaNiSn_3$-type tetragonal structure (space group is I4mm, No.

107). There are 10 atoms in the conventional unit cell, as shown in Fig. 1. The lattice parameters are $a = 4.337$ Å, $c = 10.66$ Å, giving a c/a ratio of 2.458. When doing geometry optimization, we start with the experimental geometries and calculate the dependence of the total energy E on the volume V. For the tetragonal structure, we first calculate total energies for different volumes by fixing the c/a ratio and changing the lattice parameter a, and do a least-squares fit of the E-V curve to the third-order Birch-Murnaghan equation of state (EOS)[21],

$$E(V) = -\frac{9}{16}B_0\left[(4-B_0')\frac{V_0^3}{V^2}-(14-3B_0')\cdot \frac{V_0^{7/3}}{V^{4/3}}+(16-3B_0')\frac{V_0^{5/3}}{V^{2/3}}\right]+E_0 \quad (1)$$

with E_0 being the equilibrium energy, V_0 the equilibrium volume, and B_0' the pressure derivative of the bulk modulus B_0. Secondly, we fix the value of lattice parameter $a = 4.368$ Å at the energy minimum, and change the volume by adjusting the c/a ratio, as shown in Fig. 2. After the second EOS fit, the lattice parameters of $CeAuGa_3$ are finally determined as $a = 4.384$ Å, $c = 10.655$ Å, $c/a = 2.43$, and the equilibrium volume $V_0 = 204.75$ Å^3, which are in good agreement with the experimental data[20], as listed in Tab. 1. Among the different spin configurations of $CeAuGa_3$ (*i.e.*, non-magnetic state NM, ferromagnetic state FM, and two different AFM states), the FM structure has the lowest total energy, indicating that the ground state prefers to be ferromagnetic ordering.

Tab. 1　Calculated lattice parameters (a,c), the c/a ratio, the equilibrium volume (V_0) and relative energies (E_0) of $CeAuGa_3$, compared with previous experimental results

	a /Å	c /Å	c/a	V_0/Å^3	E_0/meV
Experimental data[20]	4.337	10.66	2.458	200.51	—
NM	4.384	10.66	2.430	204.75	41.074
FM	4.373	10.74	2.456	205.41	0.000
AFM1	4.365	10.78	2.470	205.41	4.248
AFM2	4.381	10.71	2.444	205.54	7.455

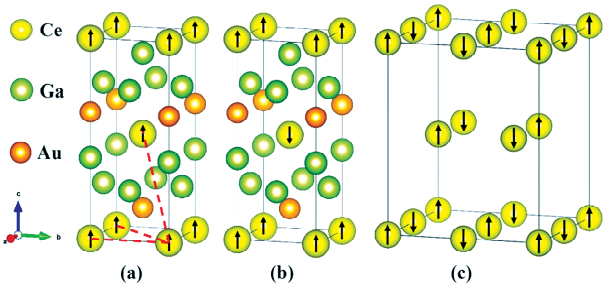

Fig. 1　Ordered spin arrangements of Ce ions in the (a) FM, (b) AFM1 and (c) AFM2 states of $CeAuGa_3$ (color online)

The red dashed lines in (a) refer to the three spin exchange paths J_1, J_2 and J_3 of Ce ions, respectively. For the ordered spin arrangement in AFM2 (c), only magnetic Ce sites are displayed for clarity in the $2 \times 2 \times 1$ supercell

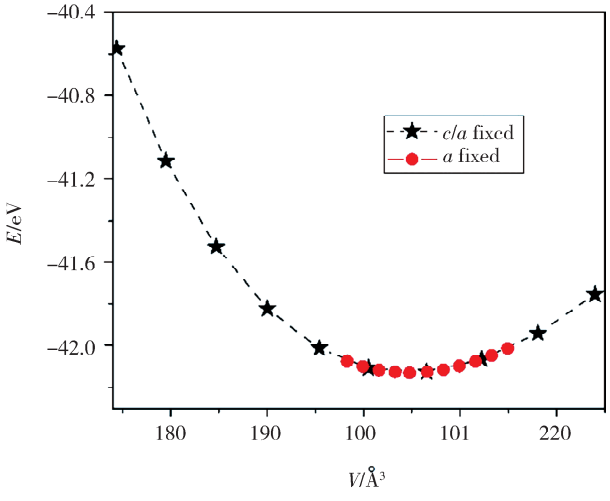

Fig. 2　The relationship between the total energy E and the unit cell volume V of $CeAuGa_3$ (color online)

The lines represent a least-squares fit to the third-order Birch-Murnaghan equation of state. The black stars denote that the data are obtained by fixing $c/a = 2.458$, and the red cycles correspond to the case of fixed $a = 4.368$ Å

Based on the total energy calculations, one may analyze the magnetic state in terms of three spin-exchange parameters, *i.e.*, the exchange coupling J_1 between the nearest-neighbour Ce ions along the $a(b)$ direction, the exchange coupling J_2 between the next-nearest-neighbour Ce ions along the diagonal path within the ab-plane, and the exchange coupling J_3 between the third-nearest-neighbour Ce ions between the adjacent $//ab$ layers, as denoted in Fig. 1(a). To extract the values of the spin-exchange parameters, we express the total spin exchange interaction energies of the three ordered spin states in terms of

the effective Heisenberg Hamiltonian,

$$H = -\sum_{i,j} J_{ij} S_i \cdot S_j \tag{2}$$

where J_{ij} denotes the spin exchange parameter (from J_1 to J_3) for the spin exchange interaction between the spin sites i and j, S_i and S_j are the spin angular momentum operators. By applying the energy expressions obtained for spin dimers[22-24], the total spin exchange energies of the three ordered spin states can be obtained as

$$E_{FM} = E_0 - 50J_1 - 25J_2 - 50J_3 \tag{3}$$

$$E_{AFM1} = E_0 - 50J_1 - 25J_2 + 50J_3 \tag{4}$$

$$E_{AFM2} = E_0 - 175J_1 - 62.5J_2 - 200J_3 \tag{5}$$

By mapping the relative energies of the three-ordered spin states determined by first-principles calculations onto the corresponding relative energies determined from the above spin-exchange energies, one can obtain $J_1 = 0.572$ meV, $J_2 = 0.414$ meV and $J_3 = 0.043$ meV listed in Tab. 2. All the spin exchange parameters J_1, J_2, J_3 are positive, indicating ferromagnetic interactions between the Ce ions, and further supporting the ferromagnetic ground state of $CeAuGa_3$. The exchange coupling between the nearest-neighbour pairs J_1 and that of the next-nearest-neighbour pairs J_2 dominate, while the third-nearest-neighbour exchange coupling J_3 may be negligible.

Tab. 2　Ce-Ce distances associated with the spin exchange paths $J_1 \sim J_3$ of $CeAuGa_3$, and the values of $J_1 \sim J_3$ determined by mapping analysis based on the present first-principles calculations

	J_1/meV	J_2/meV	J_3/meV
Ce-Ce distance/Å	4.337	6.133	6.149
Exchange coupling	0.572	0.414	0.043

3.2　Elastic properties

For tetragonal structures, there are six independent elastic constants, *i. e.*, $C_{11} = C_{22}$, C_{12}, $C_{13} = C_{23}$, C_{33}, $C_{44} = C_{55}$, and C_{66}. Under small deformations, the total energy E of a crystal associated with a strain $\mathbf{e}$ can be expressed as follows:

$$E(\mathbf{e}) = E_0 + \frac{V_0}{2}\sum_{i,j} C_{ij} e_i e_j \tag{6}$$

where e_i and e_j are components of the strain $\mathbf{e} = (e_1, e_2, e_3, e_4, e_5, e_6)$. According to Eq. (6), all the elastic constants C_{ij} can be deduced by fitting the strain energy for particular deformations. We employ six different strain states for elastic constants calculations as listed in Tab. 3. For each strain type, 14 symmetric values of strains from $\delta = -0.0175$ to 0.0175 are taken to make the strain energy fit with a step of 0.0025. The corresponding energy-strain data is shown in Fig. 3, and the calculated elastic constants are summarized in Tab. 4.

Tab. 3　Strain states used to determine the elastic constants of $CeAuGa_3$

	Strain state	$\Delta E/V_0$ to $O(\delta^2)$
1	$\mathbf{e} = (\delta, \delta, 0, 0, 0, 0)$	$(C_{11} + C_{12})\delta^2$
2	$\mathbf{e} = (0, 0, 0, 0, 0, \delta)$	$\frac{1}{2}C_{66}\delta^2$
3	$\mathbf{e} = (0, 0, \delta, 0, 0, 0)$	$\frac{1}{2}C_{33}\delta^2$
4	$\mathbf{e} = (0, 0, 0, \delta, \delta, 0)$	$C_{44}\delta^2$
5	$\mathbf{e} = (\delta, \delta, \delta, 0, 0, 0)$	$(C_{11} + C_{12} + 2C_{13} + \frac{C_{33}}{2})\delta^2$
6	$\mathbf{e} = (0, \delta, \delta, 0, 0, 0)$	$(\frac{C_{11}}{2} + C_{13} + \frac{C_{33}}{2})\delta^2$

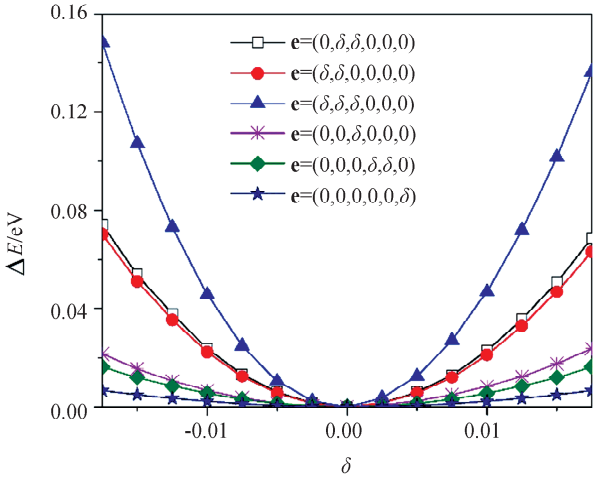

Fig. 3　Energy-strain data for $CeAuGa_3$, lines connecting data points are shown to guide the eye only(color online)

Tab. 4　The calculated elastic constants C_{ij}, bulk modulus B, shear modulus G, Young's modulus Y and Poisson's ratio ν of $CeAuGa_3$

C_{11}/GPa	C_{12}/GPa	C_{13}/GPa	C_{33}/GPa	C_{44}/GPa	C_{66}/GPa	B/GPa	G/GPa	Y/GPa	ν
118.76	54.96	69.11	114.90	42.09	33.84	70.53	11.07	31.55	0.43

One can find that all the predicted elastic constants fulfill the well-known Born-Huang stability criteria[25],

$$C_{11}-C_{12}>0 \tag{7}$$

$$C_{11}+C_{33}-2C_{13}>0 \tag{8}$$

$$C_{11}>0,\ C_{33}>0,\ C_{44}>0,\ C_{66}>0 \tag{9}$$

$$2C_{11}+C_{33}+2C_{12}+4C_{13}>0 \tag{10}$$

which confirms that $CeAuGa_3$ is mechanically stable. We have also checked the dynamical stability by the full phonon dispersion relation calculations[26] using the small displacement method[27], as shown in Fig. 4. There are in total 15 phonon branches, and all the calculated phonon frequencies along the high-symmetry directions Γ-X-R-S_0-Γ and Γ-M-S-N-P-G-M in the Brillouin zone are positive, suggesting a dynamically stable structure.

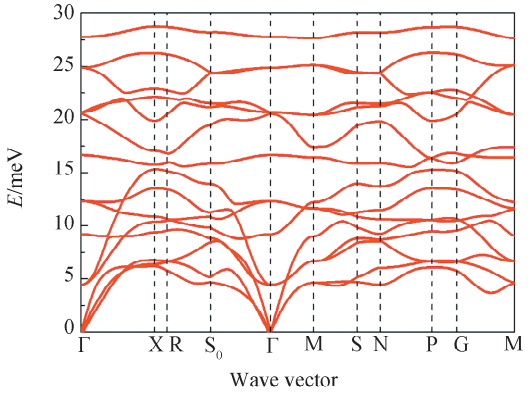

Fig. 4　Phonon dispersion curves of $CeAuGa_3$ along high symmetric directions

Based on the obtained six single-crystal elastic constants of $CeAuGa_3$, one can further obtain its polycrystalline average isotropic bulk modulus B and shear modulus G according to the Voigt-Reuss-Hill approximation[28-30]:

$$B=\frac{B_V+B_R}{2},\ G=\frac{G_V+G_R}{2} \tag{11}$$

$$B_V=\frac{2C_{11}+C_{33}+2C_{12}+4C_{13}}{9} \tag{12}$$

$$G_V=\frac{2C_{11}+C_{33}-C_{12}-2C_{13}+6C_{44}+3C_{66}}{15} \tag{13}$$

$$B_R=\frac{C_{11}+C_{12}C_{33}-2C_{13}^2}{C_{11}+C_{12}+2C_{33}-4C_{13}} \tag{14}$$

$$G_R=15/[18B_V/(C_{11}+C_{12}C_{33}-2C_{13}^2)+6/(C_{11}-C_{12})+6/C_{44}+3/C_{66}] \tag{15}$$

The Young's modulus Y and Poisson's ratio ν can be obtained as

$$Y=\frac{9BG}{3B+G},\ \nu=\frac{3B-2G}{2(3B+G)} \tag{16}$$

The calculated bulk modulus, the shear modulus, Young's modulus and Poisson's ratio for $CeAuGa_3$ are also summarized in Tab. 4. For polycrystalline phases, a high (low) ratio of bulk to shear modulus B/G is associated with ductility (brittleness) of the material[31]. The value of $CeAuGa_3$ is as high as 6.37, suggesting a high ductility of this compound.

4　Conclusions

Based on first-principles calculations, we have studied the structural properties for several different magnetic states of $CeAuGa_3$. The total energy comparison shows that its ground state prefers to be ferromagnetic ordering. By mapping analysis of different spin states, one can find that all the exchanges between Ce ions are positive (ferromagnetic type). The exchange coupling between the nearest-neighbour pairs and that of the next-nearest-neighbour pairs of Ce ions dominate, while the third-nearest-neighbour interaction between the Ce spins within adjacent //*ab* layers is relatively weak. In additions, we have checked the mechanical and dynamical stabilities by computing the elastic properties and phonon dispersion, respectively. Our results imply that $CeAuGa_3$ is both mechanically and dynamically stable, since all the calculated elastic constants satisfy the well-known Born-Huang stability criteria, and

without any imaginary phonon modes for all the wave vectors in the Brillouin zone.

References:

[1] Franz C, Senyshyn A, Regnat A, *et al*. Single crystal growth of CeTAl$_3$(T=Cu, Ag, Au, Pd and Pt) [J]. J Alloy Compd, 2016, 688: 978.

[2] Chlan V, Doležal P, Sgallová R, *et al*. Local atomic arrangement in LaCuAl$_3$ and LaAuAl$_3$ by NMR and density functional theory [J]. J Phys: Condens Matter, 2019, 31: 385601.

[3] Zarechnyuk O S, Kripyakevich P I, Gladyshevskij E I. Ternary intermetallic compounds with a BaAl$_4$-type superlattice [J]. Sov Phys Crystallogr, 1965, 9: 706.

[4] Moze O, Buschow K H J. Crystal structure of CeCuAl$_3$ and its influence on magnetic properties [J]. J Alloy Compd, 1996, 245: 112.

[5] Klicpera M, Javorský P, Čermák P, *et al*. Crystal structure and its stability in CeCuAl$_3$ single crystal [J]. Intermetallics, 2014, 46: 126.

[6] Nakashima M, Tabata K, Thamizhavel A, *et al*. High-pressure effect on the electronic state in CeNiGe$_3$: pressure-induced superconductivity [J]. J Phys: Condens Matter, 2004, 16: L255.

[7] Kotegawa H, Miyoshi T, Takeda K, *et al*. Pressure-induced superconductivity in CeNiGe$_3$ [J]. Physica B: Condens Matter, 2006, 378: 419.

[8] Kimura N, Ito K, Saitoh K, *et al*. Pressure-induced superconductivity in noncentrosymmetric heavy-fermion CeRhSi$_3$ [J]. Phys Rev Lett, 2005, 95: 247004.

[9] Sugitani I, Okuda Y, Shishido H, *et al*. Pressure-induced heavy-fermion superconductivity in antiferromagnet CeIrSi$_3$ without inversion symmetry [J]. J Phys Soc Jpn, 2006, 75: 043703.

[10] Muranaka T, Akimitsu J. Thermodynamic properties of ferromagnetic Ce-compound CeAgAl$_3$ [J]. Physica C, 2007, 460: 688.

[11] Adroja D T, del Moral A, de la Fuente C, *et al*. Vibron quasibound state in the noncentrosymmetric tetragonal heavy-fermion compound CeCuAl$_3$ [J]. Phys Rev Lett, 2012, 108: 216402.

[12] Thalmeier P, Fulde P. Bound state between a crystal-field excitation and a phonon in CeAl$_2$ [J]. Phys Rev Lett, 1982, 49: 1588.

[13] Thalmeier P. Theory of the bound state between phonons and a CEF excitation in CeAl$_2$ [J]. J Phys C: Solid State Phys, 1984, 17: 4153.

[14] Liu B Q, Čermák P, Franz C, *et al*. Lattice dynamics and coupled quadrupole-phonon excitations in CeAuAl$_3$ [J]. Phys Rev B, 2018, 98: 174306.

[15] Čermák P, Schneidewind A, Liu B, *et al*. Magnetoelastic hybrid excitations in CeAuAl$_3$ [J]. P Natl Acad Sci USA, 2019, 116: 6695.

[16] Kresse G, Hafner J. *Ab initio* molecular dynamics for liquid metals [J]. Phys Rev B, 1993, 47: 558 (R).

[17] Kresse G, Furthmüller J. Efficiency of *ab-initio* total energy calculations for metals and semiconductors using a plane-wave basis set [J]. Comp Mater Sci, 1996, 6: 15.

[18] Kresse G, Furthmüller J. Efficient iterative schemes for *ab initio* total-energy calculations using a plane-wave basis set [J]. Phys Rev B, 1996, 54: 11169.

[19] Togo A, Tanaka I. First principles phonon calculations in materials science [J]. Scripta Mater, 2015, 108: 1.

[20] Mock S, Pfleiderer C, Löhneysen H v. Low-temperature properties of CeTAl$_3$(T=Au, Cu, Pt) and CeAuGa$_3$ [J]. J Low Temp Phys, 1999, 115: 1.

[21] Birch F. Finite elastic strain of cubic crystals [J]. Phys Rev, 1947, 71: 809.

[22] Dai D, Whangbo M H. Spin-Hamiltonian and density functional theory descriptions of spin exchange interactions [J]. J Chem Phys, 2001, 114: 2887.

[23] Dai D, Whangbo M H. Spin exchange interactions of a spin dimer: analysis of broken-symmetry spin states in terms of the eigenstates of Heisenberg and Ising spin Hamiltonians [J]. J Chem Phys, 2003, 118: 29.

[24] Tian C, Lee C, Xiang H, *et al*. Magnetic structure and ferroelectric polarization of MnWO$_4$ investigated by density functional calculations and classical spin analysis [J]. Phys Rev B, 2009, 80: 104426.

[25] Born M, Huang K. Dynamical theory of crystal lattices [M]. New York: Oxford University Press, 1998.

[26] Song Y, Xu B, Nan C W. Lattice and spin dynamics in multiferroic BiFeO$_3$ and RMnO$_3$ [J]. Nat Sci Rev, 2019, 6: 642.

[27] Alfè D. PHON: A program to calculate phonons using the small displacement method [J]. Comput Phys Commun, 2009, 180: 2622.

[28] Reuss A. Berechnung der fließgrenze von mischkristallen auf grund der plastizitätsbedingung für

einkristalle [J]. Z Angew Math Mech, 1929, 9: 49.
[29] Hill R. The elastic behaviour of a crystalline aggregate [J]. Proc Phys Soc A, 1952, 65: 349.
[30] Voigt W. Lehrbuch der kristallphysik [M]. Leipzig: Teubner Press, 1928.
[31] Pugh S F. XCII. Relations between the elastic moduli and the plastic properties of polycrystalline pure metals [J]. Philos Mag, 1954, 45: 823.

引用本文格式：
中　文：程耀世，刘本琼. $CeAuGa_3$的力学性质及磁性的第一性原理计算[J]. 四川大学学报：自然科学版，2021，58：054005.
英　文：Cheng Y S, Liu B Q. Mechanical and magnetic properties of $CeAuGa_3$ from first-principles calculations [J]. J Sichuan Univ: Nat Sci Ed, 2021, 58: 054005.